SSRG International Journal of Mechanical Engineering
ISSN: 2348-8360/ https://doi.org/10.14445/23488360/IJME-V13I11P102

Volume 13 Issue 11, 9-24, November 2026
© 2026 Seventh Sense Research Group®

Original Article

Development of Quantitative Decision Framework for Welding Process Selection in Marine Fabrication using Statistical and Simulation Methods

J Anjaneyulu[1], M Venkata Ramana[2], CH V K N S N Moorthy[3], Jogula Vijay Kumar[4]

[1, 3, 4]*Department of Mechanical Engineering, Vasavi College of Engineering, Hyderabad, Telangana, India.*
[2]*Department of Mechanical Engineering, VNRVJIET, Hyderabad, Telangana, India.*

[3]*Corresponding Author: krishna.turbo@gmail.com*

Received: 28 July 2026 Revised: 21 November 2026 Accepted: 24 November 2026 Published: 27 November 2026

Abstract *- The welding process is the mostly used manufacturing process in shipbuilding that is influenced by various parameters like current, voltage, weld run speed and efficiency that affect the heat distribution, temperature flow and quality of the weld. In this work, the variability analysis is undertaken by implementing Montecarlo simulation in Python. This mainly incorporated the probabilistic approach by identifying various parameters that effect the weld quality and optimal parameters selection. Thermal analysis is performed using Finite element analysis software ANSYS for exploring temperature distribution, heat flow rates in the welded joints that are involved in shipbuilding. The marine structural components eg. web frame, stiffeners, plates and shells, are modelled using CAD software SolidWorks to understand their practical relevance. The finite element analysis software is used for transient thermal analysis to establish the temperature distribution and thermal flux flow in the ship components. The integration of numerical simulation, structural application and statistical modelling can be utilized for development of decision framework which can be used for choosing efficient welding processes that is adopted for shipbuilding. The method that is to be proposed can improve reliability by considering variability, and that will be formed a basis for improving productivity as manual intervention during fabrication is prevented.*

Keywords *- Shipbuilding, Monte-Carlo simulation, Variability analysis, Statistical modeling, Welding, Decision framework.*

1. Introduction

Shipbuilding is a multidisciplinary engineering activity which comprises the design, fabrication, assembly, installation of marine structures. The ship components like bulkheads, stiffeners, plates, vessels involve applications of principles of Mechanical engineering, Materials engineering, Welding technology, etc. Welding is crucial process that is extensively used in fabrication and assembly in shipbuilding. Various weld-type joints, like T-joints, corner joints, butt joints, are needed to be used in fabrication. Hence, the strength of these welded joints plays a vital role in the fabrication of ship. In modern manufacturing of shipbuilding, it is essential to ascertain the reliability, efficiency, safety requirements. Automation in welding has become necessary for obtaining higher efficiency and accuracy, and also to limit manual intervention. In current industries like automobile manufacturing, the use of extensive welding robots is in place as they are highly effective for welding geometries of similar batch production. Unlike the automobile industry, ships have superstructures, and especially when dealing with custom requirements of naval and marine operations, the design is subjected to be of various kinds. The Collaborative Robots (Co-Bots) are heavily tested using years of data modelling, programming and multiple phases of rollouts and updates. The automotive manufacturing industry demonstrates the potential of data-driven manufacturing, where extensive process data, programming, rigorous testing, and continuous technological development have enabled highly automated welding operations, including robotic and collaborative welding systems for complex structural assemblies. A similar transition in shipbuilding requires systematic collection and modelling of fabrication data to understand the constraints and variability associated with marine structures and welding operations. The present work provides a foundational step towards this transition by establishing a quantitative approach for analyzing welding-process performance and identifying where mechanized or semi-automated processes can be practically deployed within existing fabrication constraints. The resulting process data and decision models can further serve as a foundation for future digital-twin and AI-based manufacturing systems, enabling progressively autonomous process selection as additional data, validation, and technological capabilities become available. The

This is an open access article under the CC BY-NC-ND license (http://creativecommons.org/licenses/by-nc-nd/4.0/)

selection of type of welding is a challenging task by considering all the parameters like materials, size, location and strength, etc. The main factors to be considered in the selection of type of welding involve cost, manual intervention and quality requirements. The welding parameters such as current, voltage, speed, and heat input must be selected carefully to get a good weld. This supports the idea that process optimization can reduce defects, improve repeatability, and save time during fabrication [1]. Robotic welding can improve repeatability and consistency, while manual welding may still be better for flexible or small-batch work [2]. Welding optimization is necessary for better productivity, lower defects, and stronger ship structures [3]. Experiments help to confirm real weld behaviour, while simulation helps predict how the weld will behave before actual production [4]. Process optimization is needed even in autonomous systems, because machine control, movement accuracy, and welding conditions all affect the final result [6]. The papers [7-9] discussed the various welding techniques and the optimization of welding processes in shipbuilding.The literature survey indicated a need for a systematic and quantitative approach for welding-process selection in marine fabrication, particularly for handling process variability and differences in fabrication conditions. Statistical simulation methods such as Monte-Carlo simulation can be used to model the variability of welding process parameters and predict their notable performance over repeated operating conditions. By combining these statistical outputs with efficiency, productivity, quality and other relevant performance indices, the selection of welding process can be represented through measurable decision criteria. These criteria can then be incorporated into algorithmic decision models to evaluate alternative processes and generate process-selection recommendations with reduced dependence on manual judgement. Such data-driven decision framework provides the basis for “progressive automation” or self-directed decision system when appropriate process data and constraints are provided. This foundational work provides a basis for integrating manufacturing engineering with computational intelligence, enabling process knowledge and engineering criteria to be translated into algorithmic decision systems that reduce the time required for manual evaluation and allow repetitive decision-making tasks to be performed systematically by computational programs. The Sensitivity & Scenario Analysis has been implemented in the ship building extensively [23-26].

2. Ship Building

Marine structures such as ships and offshore platforms are primarily constructed using large steel plates and structural members, which are joined together through welding processes. Welding plays a critical role in shipbuilding as it ensures structural integrity, watertightness, and strength of the vessel. Various types of welded joints, including butt joints, T-joints and corner joints, are to be analysed for structural rigidity of the ship. The

2.1. Welding Processes used in Shipbuilding

In most vessel manufacturing industries, whether small boats, speed boats, naval, commercial or passenger types, the most important design consideration is based on the operating conditions of that vessel. Whether it is operating in cold, shallow waters, Ice-breaking types, etc. But the important thing here is metallurgy, the metal plates should not corrode in any circumstances, even in the case of any internal damage or external leakage. The appropriate welding parameters are studied and implemented in shipbuilding applications [10-13].

Along with the main metals, the welds and the structure hold equal properties to hold the ship in one piece. Therefore, use of non-reactive, high-strength alloy welding processes are used to build the blocks of the ships in modular fabrication types. The main welding processes that are discussed here are Flux-Cored Arc Weld (FCAW), Gas Metal Arc Welding (GMAW) (for Outfitting purposes), Shielded Metal Arc Welding (SMAW), and Submerged Arc Welding (SAW). Other welding processes are used in different applications.

2.2. Main Components of a Ship

Figure 1 shows some of the main components of a ship.

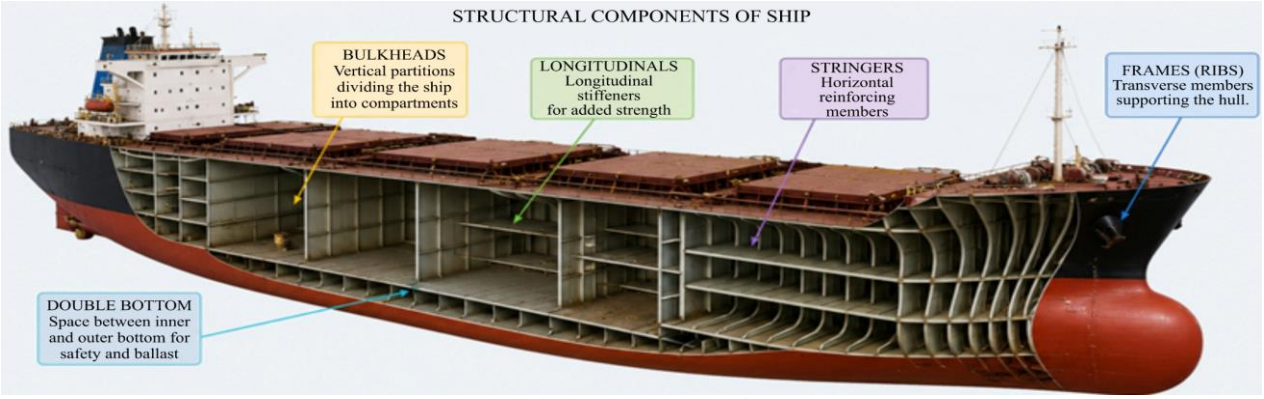


Fig. 1 Structural components of a ship

The keel is the primary longitudinal Backbone of a ship, running along the center of the bottom of the hull from the stem to stern. The Hull is a primary structural body of the ship, meaning that its forming outer shell is key in providing buoyancy, strength and hydrodynamic shape. Shell plating is the entire outer skin of a ship's hull, providing watertight integrity and longitudinal strength. Girders in a ship are primary longitudinal or transverse structural members that provide essential strength, rigidity, and stability to the hull and deck framework. Stiffeners are linear members running either longitudinally (along the ship's length) or transversely (across the ship's breadth) that are welded or riveted to the primary plates. Web frames are heavy, deep transverse frames built-up from a vertical plate web and a horizontal face flat (flange), designed to provide extra strength and rigidity to the hull cross-section. Bulkhead in a ship is an upright vertical wall (partition plate) built inside the hull to divide the ship's interior into separate rooms, tanks, and compartments. Pillar in ship structure is a vertical or near-vertical compression member that connects the upper deck (or hatch side girder) to the tank top (inner bottom) to carry deck loads down to the hull's bottom structure. Bracket is a connecting plate (usually triangular or L-shaped) used to join two or more structural members rigidly at an angle, such as beam-frame, beam-bulkhead, or stiffener-deck.

2.3. Materials

The material mostly used for ship structures is made up of mild and high-tensile marine structural steel that is used for hull and frames. This is preferred because of its excellent weldability, strength and ability to make into long box structures easily. The lighter materials like aluminium or thinner steels are used for superstructure on the decks. For piping systems, valves and pumps, stainless steel or copper alloys are used. Medium- to high-strength ship steels are used in the bow and midship areas for carrying cargo weights and are likely to be subjected to wave loads.

Stainless steel is particularly used to resist aggressive chemicals and oils being carried by ships. Nickel-based alloys and specialized copper alloys also used for heat exchangers, pumps, valves that handle hot or corrosive liquids. Zinc anodes and protective coatings are used for hull to mitigate corrosion and improve service life of the ship.

3. Welding Process Modelling and Performance Parameters

Visualization and improvisation using CAD and simulation tools allow engineers to see a design in 3D before it is built and then quickly test and improve it under realistic conditions. With CAD software, you can create detailed models of ship components, assemblies, and entire structures, making it easier to check fit, clearances, and manufacturability.

Simulation tools then let you run virtual tests-such as stress, deflection, vibration, or fluid flow analyses-to identify weak points and optimize geometry, materials, or supports without making physical prototypes. This combination of visualization and simulation speeds up design cycles, reduces errors, and helps you explore creative improvements in a safe, digital environment.

3.1. Weld Geometry Integration using Modelling Software

The weld geometry, by giving weldments in SolidWorks software, is created after modelling the individual parts, e.g, plates, brackets, web frame. The whole assembly/part, along with weldments, will be exported to Analysis software for performing transient analysis in further stages. The main weldments are classified into three types:

1. Butt weld
2. T-joint weld
3. Corner weld

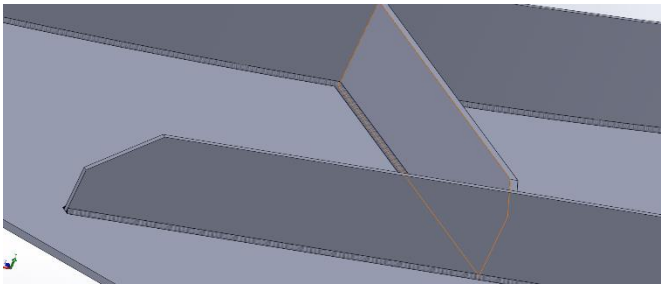


Fig. 2 T-Joint weld structure in a ship

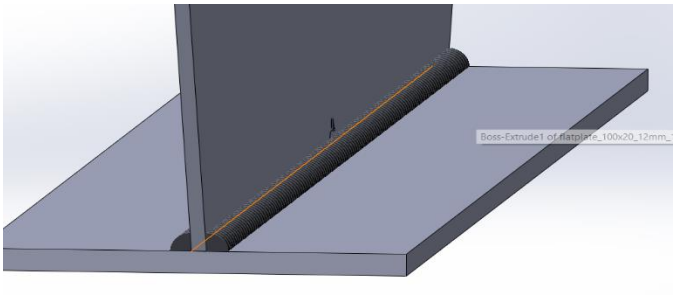


Fig. 3 Weld bead geometry made using fillet bead in SolidWorks

3.2. Transient Thermal Analysis

Thermal transient analysis is performed on the weld geometry using Ansys workbench to simulate the optimal arc time and to study thermal effects of the welding arc. This is for understanding core thermal concepts and to simulate it digitally using real data taken from the working shop floor of this shipyard fabrication facility. Finite element analysis has been extensively implemented in the estimation of welded structures' behaviour [20-22].

Transient analysis tracks the weld torch's movement, revealing how heat input propagates through the plate geometry over time. This identifies peak temperatures (often

>1500°C for steel), Heat-Affected Zone (HAZ) boundaries where microstructure changes occur (e.g., grain coarsening or phase transformations), and cooling rates that dictate final properties like hardness or toughness. It predicts distortions from thermal expansion/contraction cycles, residual stresses leading to cracking, and validates weld bead profiles against defects like porosity or incomplete fusion-essential for optimizing plate designs in industrial applications.

Finite element transient thermal analysis for a flat-plate butt-weld geometry is a high-fidelity numerical approach used to predict the evolution of temperature fields and the resulting residual stress and distortion during the welding process. Unlike steady-state analysis, transient analysis accounts for the time-dependent movement of the heat source (often modelled using Goldak's double-ellipsoidal heat source), allowing us to capture the rapid heating and cooling cycles that dictate the metallurgical transformation within the Heat Affected Zone (HAZ). By discretizing the geometry into a 3D mesh, typically with a refined density near the weld fusion line to capture the sharp thermal gradients and a coarser mesh in the base metal to maintain computational efficiency, non-linear heat conduction equations that incorporate temperature-dependent thermal properties such as thermal conductivity, specific heat, and density can be solved.

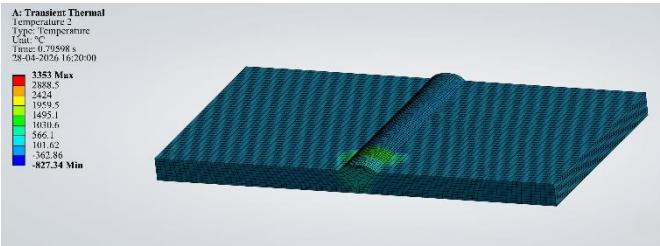


Fig. 4 Temperature plot after 0.7 seconds

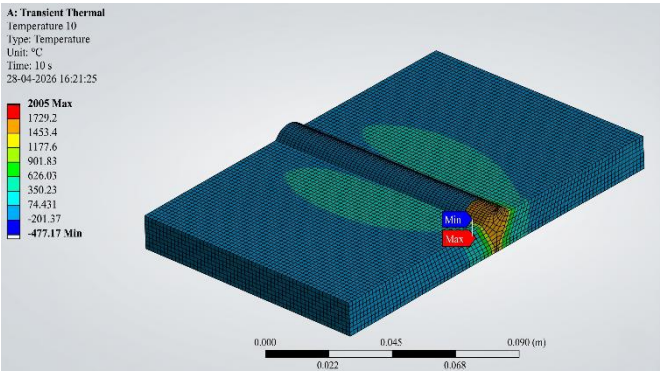


Fig. 5 Temperature plot after 10 seconds

The transient thermal behavior of the welding process was analyzed using the Goldak double-ellipsoid heat-source model, in which the welding currents, voltage and travel speed determine the heat supplied and its movement along the weld path. The effective heat input to the workpiece was calculated using the arc efficiency and electrical welding parameters as:

$$HI = \frac{\eta VI}{v}$$

Where HI is the heat input per unit weld length (J/mm), $\eta$is the arc efficiency, $V$is the welding voltage (V), $I$is the welding current (A), and $v$is the welding speed (mm/s). The calculated heat input was used as the basis for defining the moving heat source in the transient thermal analysis, allowing the resulting temperature distribution and thermal response of the welded region to be evaluated for the selected welding conditions.

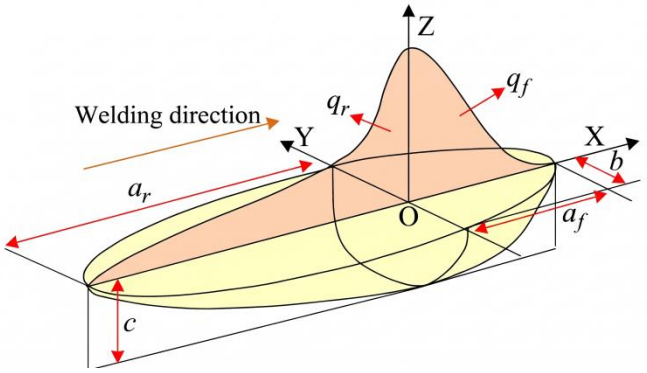


Fig. 6 Goldak double-ellipsoid heat-source model

[10] From the paper, this is a model of Goldak double ellipsoid.

The transient moving heat source can be represented by two ellipsoidal regions: a front region and a rear region. The volumetric heat-source distributions are:

$$q_f(x, y, z, t) = \frac{6\sqrt{3} f_f Q}{a_f bc\pi\sqrt{\pi}} \exp[-3(\frac{x'^2}{a_f^2} + \frac{y^2}{b^2} + \frac{z^2}{c^2})]$$

$$q_r(x, y, z, t) = \frac{6\sqrt{3} f_r Q}{a_r bc\pi\sqrt{\pi}} \exp[-3(\frac{x'^2}{a_r^2} + \frac{y^2}{b^2} + \frac{z^2}{c^2})]$$

Where $a_f$and $a_r$define the front and rear longitudinal dimensions, while $b$and $c$define the transverse and depth dimensions of the heat source. The front/rear fractions satisfy:

$$f_f + f_r = 2$$

The moving coordinate can be expressed as:

$$x' = x - vt$$

So, welding speed directly controls the movement of the heat source through the model.

The results are based on the data file utilised while running the code in this case. The firmly recorded and documented welding processes that are real values are FCAW Manual, SAW, Flux Track (FT), CoBot, etc. The welding processes strictly adhering to stick with FCAW-G ('G' represents shielding gas, mostly CO_2) and the coil used for welding is E601 T5-GM, can be observed to give basic slag after welding and for a smooth arc. It produces radiographic-quality welds with very low level of hydrogen (H4) and is a superior coil used to fabricate welds suitable with HSLA steel. A special coil specifically manufactured for naval ship welding applications. Therefore, the data collected in the timeframe of my observations in Shop floor, most processes are either stick welding (mostly used for fit-up and support structures), hence ruled out from our simulation, as our primary focus is on improvement of arc time and time-study of major welding processes, comparing both manual labour against the production quality of auto/semi-auto (mechanised) processes.

Below are the main processes that are used in my observation and are best-case utilisation for that standard.

Table 1. Welding process classification

Welding process	Type
Flux-Track (Semi-auto)	FCAW-G/ GMAW
Cobot (Auto/Semi-auto)	FCAW-G/ GMAW
SAW (Semi-auto)	FCAW
Manual Labour	FCAW/GMAW/ SMAW, etc
MOGI Tractor (Auto)	FCAW/ GMAW

An important highlight is that any wire feed process can be both FCAW & GMAW, provided that their use cases are different, and GMAW specifically need shielding gas to operate. FCAW works with or without shielding gas based on its application and wire type. So, understanding the graphs at basic level is necessary, hence only bar plots are used to compare all the processes, efficiencies and RT rates.

4. Quantitative Decision Framework for Welding Process Selection

A quantitative decision framework is a systematic, data-driven methodology that uses mathematical models, statistics, and numerical analysis to evaluate alternatives and make objective decisions, rather than relying on intuition or experience alone.

The core characteristics:

- Numbers-Based: Converts all decision factors into measurable values (rates, costs, probabilities, scores)
- Mathematical Models: Uses formulas like weighted sums, optimization functions, or simulations
- Reproducible: Same inputs always produce same outputs
- Transparent: Shows exactly how each decision factor contributes to final ranking

This clearly means that the data itself is the foundation for a strong quantifiable decision framework. Then it is a definite, measurable parameter. If welding data is data-driven rather than intuition- and experience-based, then it is a leap forward to integrate future welding processes with complete automation and Artificial intelligence and Machine Learning concepts. The present-day Co-Bots are already the most efficient machines for welding tight spaces, and reduced human interference can help us achieve better-quality welds. As long as skilled labour is present, welding manually also makes sense, as their expertise know and can find out penetration during arc and rectify the weld bead with proper arc.

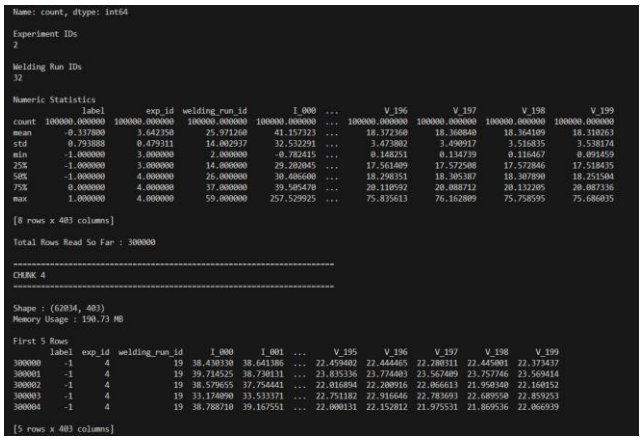
Therefore, manual labour cannot be completely ruled out, because it is very crucial to have manual labour for rework weld beads, repairing work on ships, and other welding needs where robots cannot help. But, meanwhile, automation has reduced strain on human effort and increased efficiency. For example, processes like Seamless Arc Welding (SAW) are very useful for sheet joining, panel welding and side shell welding. SAW is used for longer thick weld beads, and they are the most accurate welding techniques commonly used in heavy engineering work. The advantage is that it doesn't require a shielding gas but only requires filler dust. The "sand" used in Submerged Arc Welding (SAW) is actually granular flux, a mineral compound that acts as a shielding agent. It protects the molten weld metal from atmospheric contamination, stabilizes the arc, and acts as a deoxidizer. This granular flux is gravity-fed in a thick blanket ahead of the welding arc. Contains oxides of manganese, silicon, titanium, aluminium, calcium, magnesium, and fluorides. To optimize our welding production, a data-driven decision framework is developed that shifts our process selection from intuition-based choices to a structured, performance-based model. By classifying all structural connections into three core categories:

- T-joints
- butt joints
- corner joint

It is established a baseline that allows us to leverage the insights gained from our Monte Carlo simulations. These simulations have provided us with a high-fidelity understanding of the probability density for productivity and quality across our entire shop floor, revealing that certain processes, while highly efficient for specific joint geometries, can become bottlenecks when applied to others due to setup-time volatility or heat-input constraints. Our framework systematically evaluates each joint type against our critical KPIs-specifically targeting an increase in arc-on time, a reduction in rework through improved Radiographic (RT) pass rates, and an overall optimization of energy input to protect the metallurgical integrity of the HSLA material.

For instance, in applications where the simulation indicates high variability in setup time, the framework directs the project toward processes that minimize non-value-added logistics, while for critical structural joints identified as having high sensitivity to heat input, the processes are prioritized that offer the most stable thermal control. By integrating this framework into the required daily operations, a welding machine is not chosen, but by aligning the required process capabilities with the specific geometric and structural demands of each connection, only the particular welding machine is chosen.

Ultimately, this decision framework serves as a roadmap for the crew, providing them with the necessary technical guidance to select the right tool for the right joint, ensuring that every weld produced meets the stringent standards required for naval applications while simultaneously driving the shop floor toward its maximum potential for productivity and quality [14-19]. Chunk breakdown method used in python to take a bunch of values at a time, as shown in Figures 7 to 9. This method is used when the access file contains very large number of values and cannot be readable due to its merging techniques. Zenodo [11] provides a python function that helps us make the data readable.



```
Name: count, dtype: int64

Experiment IDs
2

Welding Run IDs
32

Numeric Statistics
              label         exp_id  welding_run_id          I_000  ...          V_196          V_197          V_198          V_199
count  100000.000000  100000.000000   100000.000000  100000.000000  ...  100000.000000  100000.000000  100000.000000  100000.000000
mean        -0.337800       3.642350       25.971260      41.157323  ...      18.372360      18.360840      18.364109      18.310263
std          0.793888       0.479311       14.002937      32.532291  ...       3.473802       3.490917       3.516835       3.538174
min         -1.000000       3.000000        2.000000      -0.782415  ...       0.148251       0.134739       0.116467       0.091459
25%         -1.000000       3.000000       14.000000      29.202045  ...      17.561409      17.572508      17.572846      17.518435
50%         -1.000000       4.000000       26.000000      30.486640  ...      18.298351      18.305387      18.307898      18.251504
75%          0.000000       4.000000       37.000000      39.585470  ...      20.110592      20.088712      20.132205      20.087336
max          1.000000       4.000000       59.000000     257.529925  ...      75.835613      76.162889      75.758595      75.686035

[8 rows x 403 columns]

Total Rows Read So Far : 300000

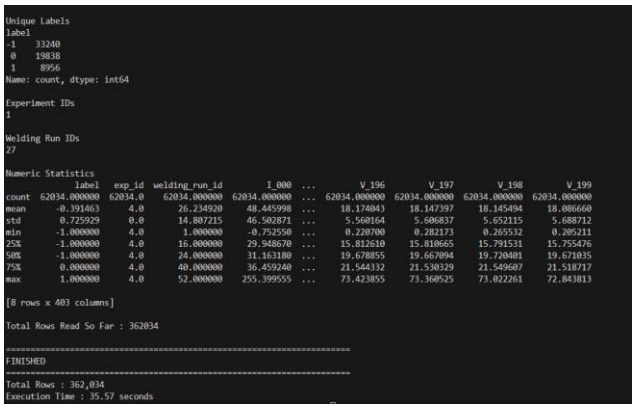
--------------------------------------------------------------------------------
CHUNK 4
--------------------------------------------------------------------------------

Shape : (62034, 403)
Memory Usage : 190.73 MB

First 5 Rows
        label  exp_id  welding_run_id      I_000      I_001  ...      V_195      V_196      V_197      V_198      V_199
300000     -1       4              19  38.430330  38.641386  ...  22.459482  22.444465  22.280311  22.445001  22.373437
300001     -1       4              19  39.714525  38.730121  ...  23.835336  23.774403  23.567409  23.757746  23.569414
300002     -1       4              19  38.579655  37.754441  ...  22.016894  22.200916  22.066613  21.950340  22.168152
300003     -1       4              19  33.174090  33.533371  ...  22.751182  22.916646  22.783693  22.689550  22.859253
300004     -1       4              19  38.788710  39.167551  ...  22.000131  22.152812  21.975531  21.869536  22.066939

[5 rows x 403 columns]
```

Fig. 7 Statistical summary and chunk-wise processing of the experimental dataset



```
Unique Labels
label
-1    33240
 0    19838
 1     8956
Name: count, dtype: int64

Experiment IDs
1

Welding Run IDs
27

Numeric Statistics
              label   exp_id  welding_run_id          I_000  ...          V_196          V_197          V_198          V_199
count  62034.000000  62034.0    62034.000000   62034.000000  ...  62034.000000  62034.000000  62034.000000  62034.000000
mean      -0.391463      4.0       26.234920      48.445998  ...     18.174043     18.147397     18.145494     18.086660
std        0.725929      0.0       14.807215      46.502871  ...      5.560164      5.606837      5.652115      5.688712
min       -1.000000      4.0        1.000000      -0.752550  ...      0.220700      0.282173      0.265532      0.205211
25%       -1.000000      4.0       16.000000      29.948670  ...     15.812610     15.810665     15.791531     15.755476
50%       -1.000000      4.0       24.000000      31.163180  ...     19.678855     19.667094     19.720401     19.671035
75%        0.000000      4.0       40.000000      36.459240  ...     21.544332     21.530329     21.549607     21.518717
max        1.000000      4.0       52.000000     255.399555  ...     73.423855     73.360525     73.022261     72.843813

[8 rows x 403 columns]

Total Rows Read So Far : 362034

================================================================================
FINISHED
--------------------------------------------------------------------------------
Total Rows : 362,034
Execution Time : 35.57 seconds
```

Fig. 8 Final dataset summary, class distribution, and data processing statistics.

	A	B	C	D	E	F	G	H	I	J	K
1	Process	Mode	Meters_per_Hour	RT_Pass_Fail	Plate_Thickness_mm	Labour_Cost_Index	Voltage_V	Current_A	Setup_Time_min	Cleaning_Time_min	Arc_Time_min
2	CoBot	Automated	21.869	pass	12	Low	31.559	343.874	7.458	3.8	2.851
3	CoBot	Automated	21.338	Pass	12	Low	30.041	358.796	11.324	4.699	2.518
4	CoBot	Automated	19.384	Pass	14	Low	30.014	320.922	8.248	6.199	2.356
5	CoBot	Automated	29.659	Pass	14	Low	31.57	327.987	8.142	7.739	2.356
6	CoBot	Automated	24.898	Pass	12	Low	30.027	357.688	8.633	6.083	2.319
7	CoBot	Automated	20.002	Pass	14	Low	30.244	339.807	3.344	10.275	2.611
8	CoBot	Automated	25.613	Pass	14	Low	30.416	342.708	3.313	9.738	2.84
9	CoBot	Automated	22.137	Fail	12	Low	31.844	323.54	4.96	3.362	2.69
10	CoBot	Automated	22.053	Pass	12	Low	31.174	358.61	9.07	5.208	2.656
11	CoBot	Automated	19.148	Pass	12	Low	31.544	327.949	3.055	9.524	3.148
12	CoBot	Automated	26.477	Pass	12	Low	31.853	346.043	12.15	9.8	2.839
13	CoBot	Automated	18.24	Pass	14	Low	30.65	349.184	9.376	10.098	2.867
14	CoBot	Automated	18.555	Pass	12	Low	31.443	329.439	5.561	3.323	3.153
15	CoBot	Automated	18.442	Pass	12	Low	30.063	345.456	6.144	7.069	3.389
16	CoBot	Automated	20.241	Pass	12	Low	30.406	357.714	8.989	8.558	3.357
17	CoBot	Automated	25.117	Pass	12	Low	31.743	352.147	4.866	10.14	2.947
18	CoBot	Automated	27.497	Pass	12	Low	31.814	330.885	9.477	3.004	2.723
19	CoBot	Automated	20.962	Pass	12	Low	30.835	328.884	4.199	5.701	3.431
20	CoBot	Automated	21.202	Pass	12	Low	30.808	322.596	5.539	4.975	3.136
21	CoBot	Automated	26.26	Pass	14	Low	30.074	344.383	8.027	3.412	2.634
22	FT	semi_auto	19.541	Pass	5	Medium	24.29	167.342	8.914	3.69	4.484
23	FT	semi_auto	18.361	Fail	5	Medium	24.475	170.923	5.207	3.69	5.265
24	FT	semi_auto	18.168	Pass	5	Medium	24.181	172.53	4.925	3.69	4.373
25	FT	semi_auto	15.204	Pass	5	Medium	25.355	160.249	6.073	3.69	4.453
26	FT	semi_auto	18.226	Pass	5	Medium	25.382	165.801	8.62	3.69	4.275
27	FT	semi_auto	16.705	Pass	5	Medium	25.849	173.16	4.548	3.69	5.32
28	FT	semi_auto	19.086	Pass	5	Medium	25.059	163.628	3.559	3.69	5.794
29	FT	semi_auto	19.502	Pass	5	Medium	24.678	165.238	7.356	3.69	5.794
30	FT	semi_auto	19.435	Fail	5	Medium	25.284	161.262	3.97	3.69	5.797
31	FT	semi_auto	18.032	Pass	5	Medium	24.203	169.953	3.03	3.69	4.322
32	FT	semi_auto	17.744	Pass	5	Medium	25.304	163.364	7.273	3.69	4.474
33	FT	semi_auto	16.627	Pass	5	Medium	25.299	172.738	6.946	3.69	5.137
34	FT	semi_auto	15.468	Pass	5	Medium	24.53	163.66	8.838	3.69	4.786

Fig. 9 Experimental dataset showing welding process parameters and performance metrics for CoBot and FT welding under automated and semi-automated operating modes

The primary publicly accessible data source considered in this study is a welding dataset available through the Zenodo [11] research data repository. The available dataset was used as the principal reference for the welding-process electrical parameters used in the computational analysis.

However, the publicly available data do not contain all the process variables required to construct a comprehensive Monte Carlo simulation framework, particularly parameters such as arc time, plate thickness and other process-dependent variables required for evaluating process variability and probabilistic performance.

Due to a non-disclosure agreement, without presenting or identifying any confidential industrial measurements, a representative synthetic dataset was generated using the publicly available welding data as a reference, together with comparable published welding datasets and physically meaningful parameter ranges.

The synthesized dataset was used solely to demonstrate the implementation of the Python-based Monte Carlo simulation, variability analysis and associated performance indices. This approach allows the proposed computational framework to be demonstrated and evaluated while maintaining the confidentiality of the industrial data.

5. Monte Carlo Simulation and Process Variability Modelling

Monte Carlo simulation was selected as the primary computational method as welding processes involve inherent variability in parameters such as welding time, current, voltage, travel speed and process efficiency. Instead of evaluating a process using a single value, this enables these variable parameters to be represented through probability distributions and repeatedly sampled to estimate their probable range of performance.



Fig. 10 Monte Carlo simulation: Process predictability

Mean Welding Travel Rate (m/h)

It represents the average length of weld produced per hour of arc-on welding time for a given welding process.

For each observation *i*, the individual welding travel rate is calculated as:

$$V_i = \frac{L_i}{t_i} \times 60$$

Where:

- V_i welding travel rate for observation *i*(m/h)
- L_i = weld length (m)
- t_i = arc time (min)
- 60 = conversion factor from minutes to hours

For *n* observations belonging to the same welding process, the mean welding travel rate is:

$$\bar{V} = \frac{1}{n}\sum_{i=1}^{n} V_i$$

The corresponding sample standard deviation is:

$$s_V = \sqrt{\frac{\sum_{i=1}^{n}(V_i - \bar{V})^2}{n-1}}$$

Therefore, the process result can be reported as: $\bar{V} \pm s_V$ m/h

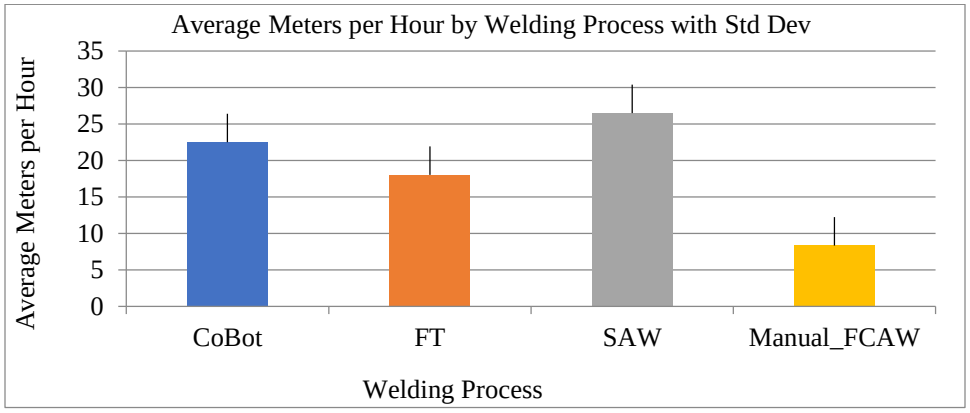


Fig. 11 Average meters per hour by welding process with standard deviation

- Average Welding Rate by Mode ± Standard Deviation (m/h).

$$\bar{V}_{mode} = \frac{\sum_{i=1}^{n} V_i}{n}$$

$$s_{V,mode} = \sqrt{\frac{\sum_{i=1}^{n}(V_i - \bar{V}_{mode})^2}{n-1}}$$

Therefore:

$$\boxed{\bar{V}_{mode} \pm s_{V,mode}}$$

- RT pass/fail rate by welding process and mode

RT Pass Rate

$$P_{pass} = \frac{N_{pass}}{N_{total}} \times 100$$

RT Fail Rate

$$P_{fail} = \frac{N_{fail}}{N_{total}} \times 100$$

Where

$$N_{total} = N_{pass} + N_{fail}$$

For a stacked chart, each welding process/mode combination therefore has:

$$P_{pass} + P_{fail} = 100\%$$

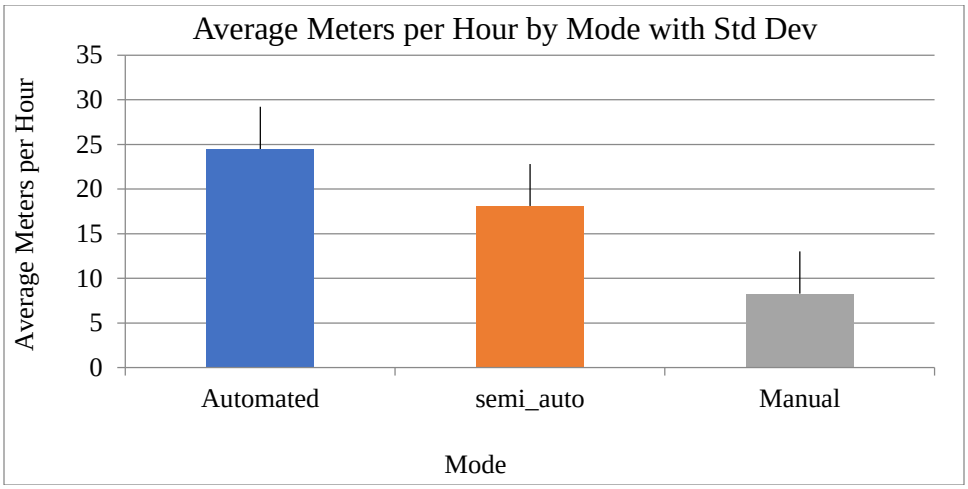


Fig. 12 Average meters per hour by mode with standard deviation

```
--- Quality Summary (RT Pass/Fail Rates %) ---
RT_Pass_Fadl      Process       Mode   Pass_Rate  Fail_Rate
0                    CoBot  Automated   90.000000   5.000000
1                       FT  semi_auto   80.000000  20.000000
2            Manual_FCAW     Manual   78.947368  21.052632
3                      SAW  Automated  100.000000   0.000000
```

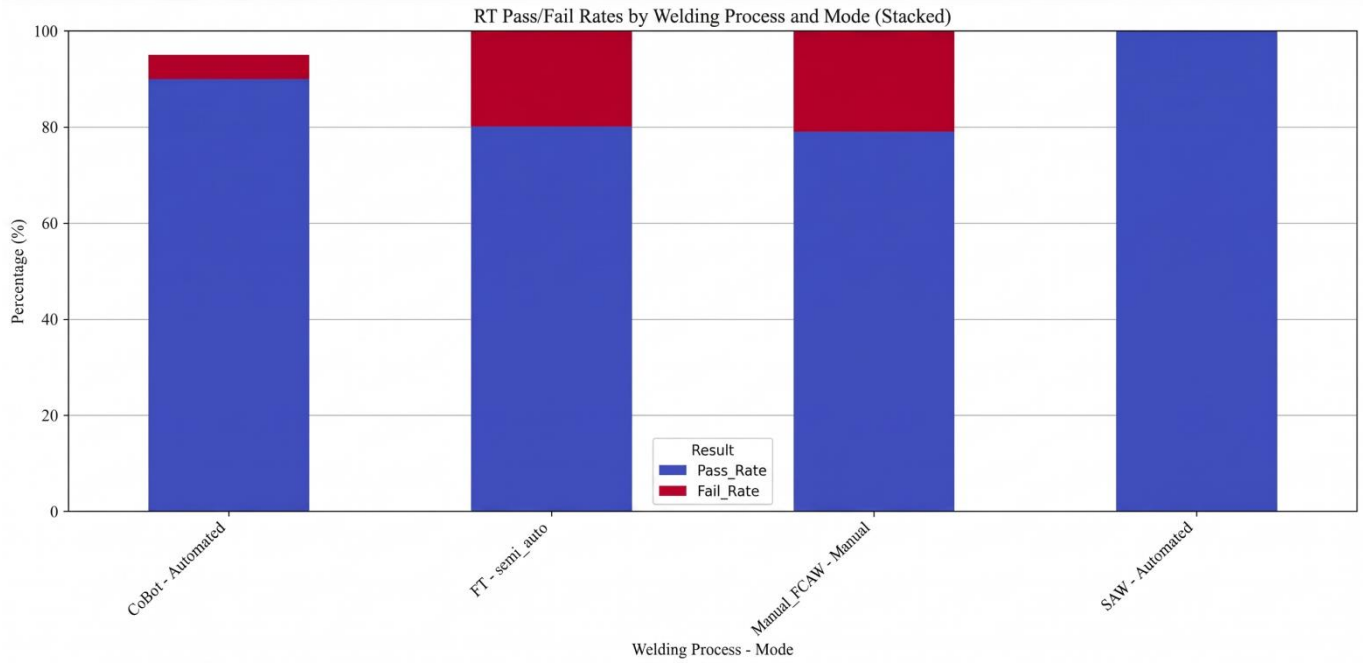


Fig. 13 RT pass/fail by welding process and mode (stacked)

- Productivity (m/hr) versus rt pass rate (%) with variability faceted by mode

  Productivity

  $P_i = \frac{L_i}{t_i} \times 60$

  Mean Productivity

  $\bar{P} = \frac{1}{n}\sum_{i=1}^{n} P_i$

  RT Pass Rate

  $R_{pass} = \frac{N_{pass}}{N_{total}} \times 100$

  Productivity Variability

  $s_P = \sqrt{\frac{\sum_{i=1}^{n}(P_i - \bar{P})^2}{n-1}}$

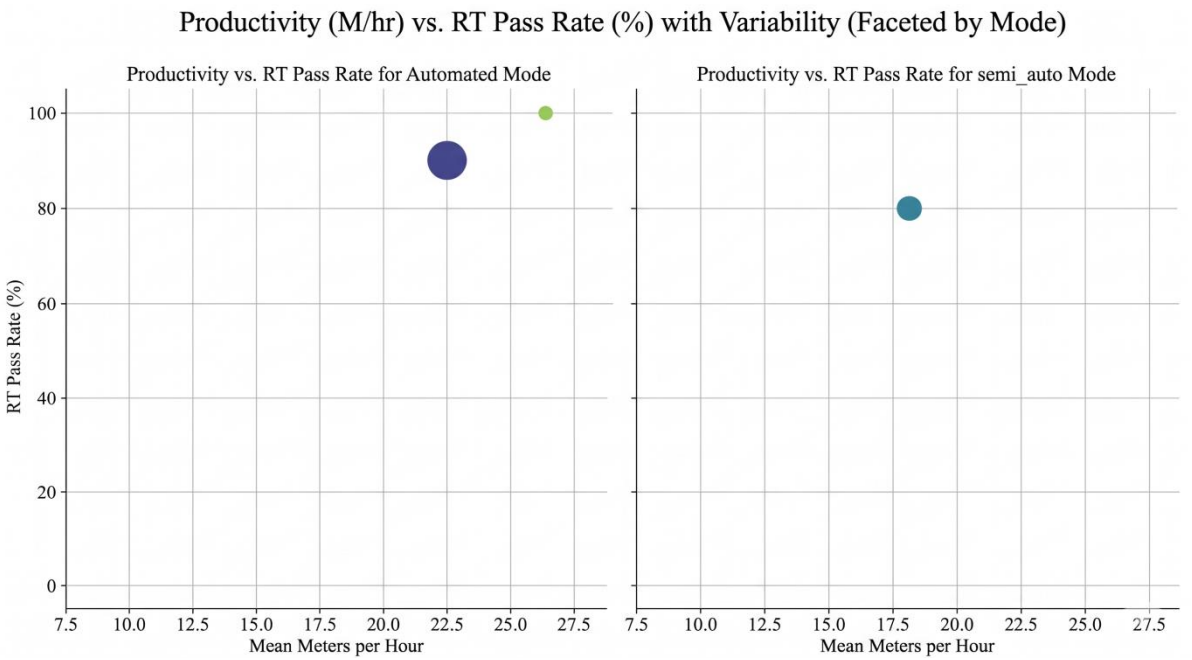


Fig. 14 Productivity (m/hr) versus RT pass rate (%) with variability faceted by mode

- Productivity (m/hr) versus plate thickness, process and mode

Productivity

$$P_i = \frac{L_i}{t_i} \times 60$$

Mean productivity for each plate thickness-process-mode combination

$$\bar{P}_{t,p,m} = \frac{1}{n}\sum_{i=1}^{n} P_i$$

So, the plotted relationship is:

$\boxed{\bar{P}_{t,p,m} \text{ vs. } T}$

Where:

- P_i= productivity of observation i(m/hr)
- L_i= weld length (m)
- t_i= welding/arc time (min)
- T= plate thickness (mm)
- p= welding process
- m= welding mode
- n= number of observations for that thickness-process-mode combination.

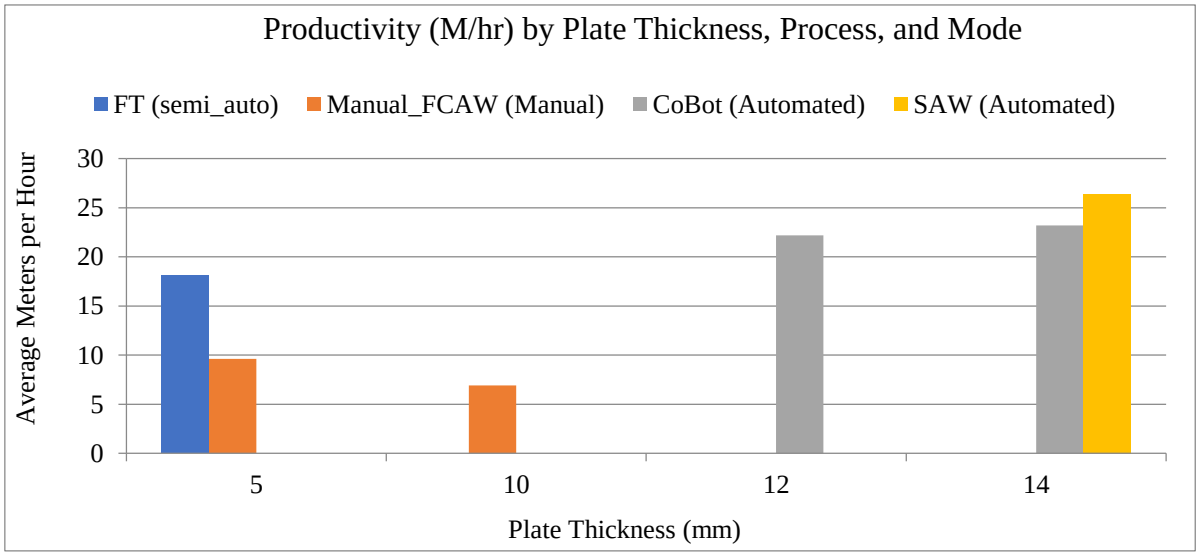


Fig. 15 Productivity (m/hr) versus plate thickness, process and mode

- Average time breakdown by process and mode(%)

Where $t_j$is the time spent in a particular activity and $t_{total}$is the total process time.

For the average percentage across $n$observations:

$$\bar{T}_j = \frac{1}{n}\sum_{i=1}^{n} T_{ij}$$

So the final parameter is:

$$\boxed{\bar{T}_j(\%)}$$

Where $j$represents the time component (welding, cleaning, setup, handling, inspection, etc.), calculated separately for each welding process and mode.

```
--- Average Time Breakdown (%) ---
      Process       Mode  Arc_Time_Pct  Cleaning_Time_Pct  Setup_Time_Pct
0       CoBot  Automated         17.15              40.04           42.81
1          FT  semi_auto         34.09              25.35           40.56
2  Manual_FCAW     Manual         39.52              24.44           36.04
3         SAW  Automated         23.10              11.33           65.57
```

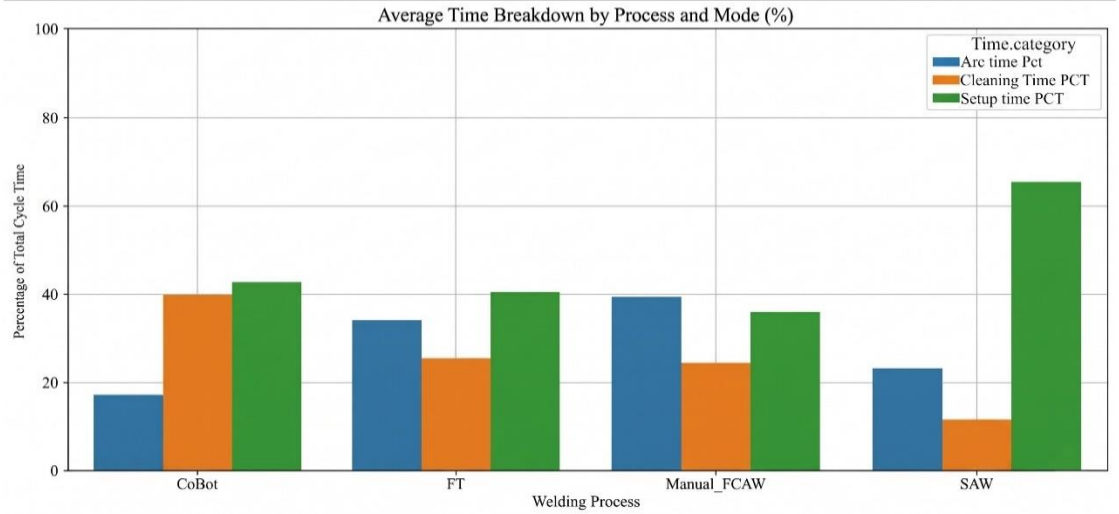


Fig. 16 Average time breakdown by process and mode (%)

- Welding efficiency index (%) by process and mode

Where $t_{weld}$is the effective welding/arc-on time and $t_{total}$is the total process time including setup, handling, cleaning, inspection, etc.

For n observations for each process and mode:

$$\overline{WEI} = \frac{1}{n}\sum_{i=1}^{n} WEI_i$$

So the reported parameter is: WEI (%)

```
--- Welding Efficiency Index (Arc-on Time / Total Cycle Time) ---
      Process       Mode  Welding_Efficiency_Index_Pct
0       CoBot  Automated                         17.15
1          FT  semi_auto                         34.09
2  Manual_FCAW     Manual                         39.52
3         SAW  Automated                         23.10
```

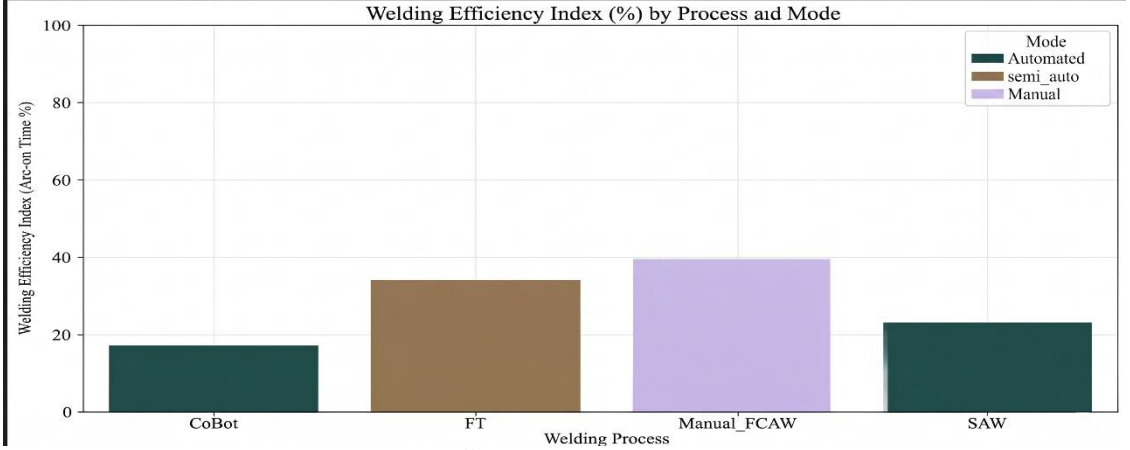


Fig. 17 Welding efficiency index (%) by process and mode

Welding efficiency here is high for manual FCAW due to its repeated output and usage. Comparing work output with other processes, Manual Labour stands as it is faster compared to setting up complex machinery on bulkhead. This is due to the limitation of automated processes operating span or limited area usage.

- Average heat input (J/mm) by process and mode with standard deviation

Where $HI_i$is heat input (J/mm), $V_i$is voltage (V), $I_i$is current (A), $\eta$is arc efficiency, and $S_i$is welding speed (mm/s).

Mean heat input:

$$\underline{HI} = \frac{1}{n}\sum_{i=1}^{n} H\, I_i$$

Standard deviation:

$$s_{HI} = \sqrt{\frac{\sum_{i=1}^{n}(HI_i - HI)^2}{n-1}}$$

Final reported value: HI ± s_{HI} (J/mm)

```
--- Heat Input Summary (J/mm) ---
      Process        Mode         mean          std          std          max
0       CoBot  Automated  1718.784546   235.781924  1256.831941  2112.333474
1          FT  semi_auto   841.919118    74.825147   748.838537   964.600193
2  Manual_FCAW      Manual  3244.725650  1380.978646  1808.831318  6100.502249
3         SAW  Automated  1856.878566    70.420864  1757.700207  2020.582935
```

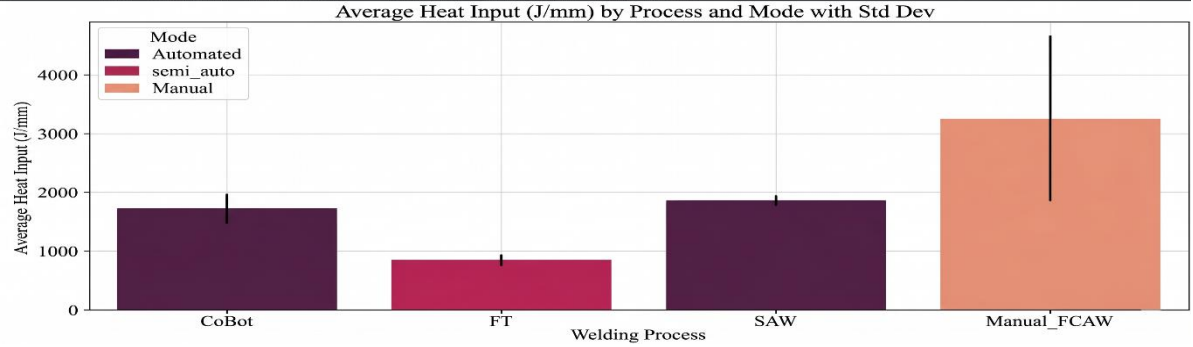


Fig. 18 Average heat input (J/mm) by process and mode with standard deviation

The maximum Heat input in observed in Manual FCAW with highest standard deviation because the welders using higher current and voltage inputs instead of standard arc requirements. Maybe because of this action, the process inconsistency, which results in highest rework factor, can be seen.

6. Cost and Productivity Analysis for Welding Process Selection

The cost and productivity of each welding process and mode were evaluated using the estimated process cost, welding time and productivity obtained from the statistical analysis. These parameters were compared to identify the relative economic and production performance of the available welding alternatives and were subsequently considered in the process suitability evaluation.

- Correlation matrix of heat input, productivity and quality

For correlation matrix, the formulation is the Pearson correlation coefficient between each pair of variables.

For variables X and Y:

$$r_{XY} = \frac{\sum_{i=1}^{n}(X_i - \bar{X})(Y_i - \bar{Y})}{\sqrt{\sum_{i=1}^{n}(X_i - \bar{X})^2 \sum_{i=1}^{n}(Y_i - \bar{Y})^2}}$$

Where r_{XY}ranges from $-1$to $+1$.

For the three variables:

$r_{HI,P}$

$r_{HI,Q}$

$r_{P,Q}$

Where:

- HI= Heat Input
- P= Productivity
- Q= RT quality/pass indicator

The matrix is therefore showing the pairwise Pearson coefficients:

- Heat Input vs Productivity: -0.5513
- Heat Input vs RT Quality: -0.2788
- Productivity vs RT Quality: 0.2532

The diagonal is always:

$r_{XX} = 1$

```
--- Correlation Matrix (Heat Input, Productivity, Quality) ---
                 Heat_Input_J_mm  Meters_per_Hour  RT_Pass_Numeric
Heat_Input_J_mm         1.000000        -0.551323        -0.277851
Meters_per_Hour        -0.551323         1.000000         0.253249
RT_Pass_Numeric        -0.277851         0.253249         1.000000
```

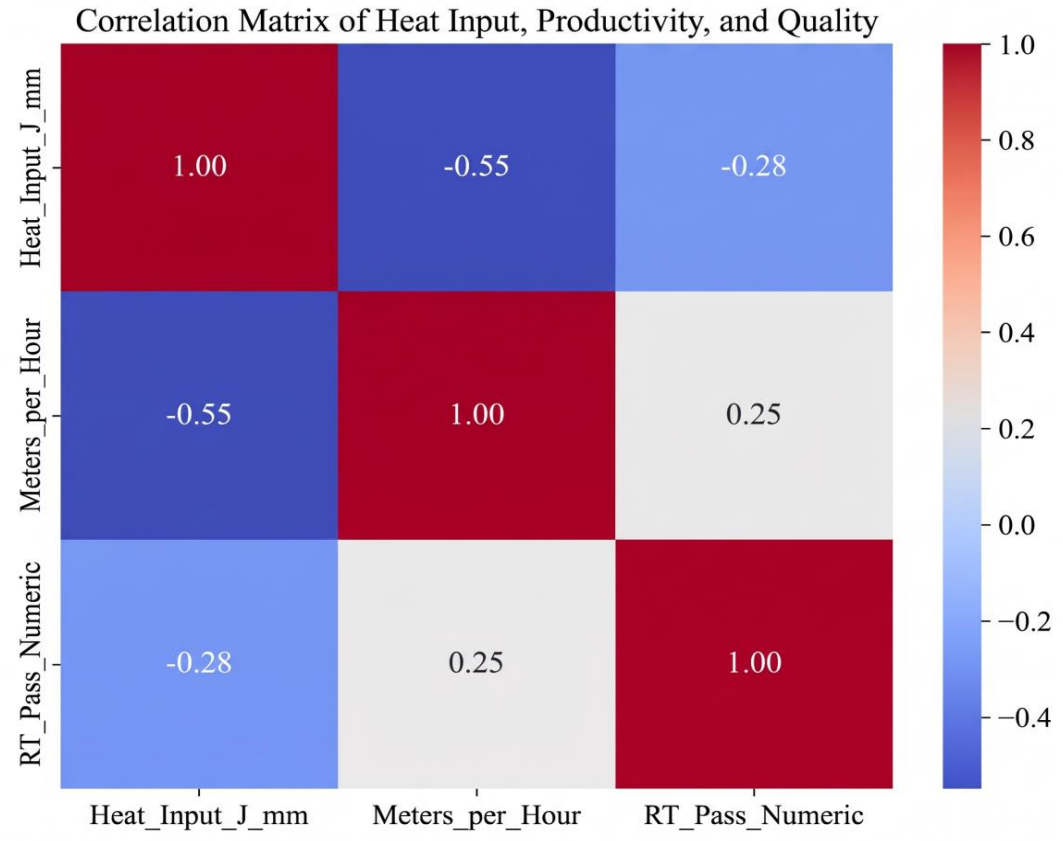


Fig. 19 Correlation matrix of heat input, productivity and quality

To optimize this process, the data suggest that increasing speed (Productivity) is a "win-win" here-it not only saves time but is also correlated with lower heat input and a higher likelihood of passing quality inspections. Higher productivity (faster speeds) is slightly associated with better quality outcomes in this dataset.

This might imply that the process is more stable at higher speeds, or that the reduced heat input associated with those speeds is beneficial for the integrity of the weld.

- Process suitability index (psi) by welding process and mode (with numeric cost)

$$PSI_{p,m} = \sum_{j=1}^{k} w_j \, R_{p,m,j}$$

Where w_j is the weight assigned to criterion j, and $R_{p,m,j}$ is the normalized performance value for process p and mode m.

For a benefit criterion such as productivity or quality:

$$R_{ij} = \frac{x_{ij}}{\max(x_j)}$$

For a cost criterion:

$$R_{ij} = \frac{\min(x_j)}{x_{ij}}$$

The numeric cost can therefore be included as a cost-type criterion:

$$R_{cost} = \frac{C_{min}}{C_{p,m}}$$

and the overall PSI becomes, for example:

$$\boxed{PSI_{p,m} = w_P R_P + w_Q R_Q + w_H R_H + w_C R_C}$$

Where C represents the cost criterion.

If higher PSI = more suitable, the process/mode combination with the highest PSI is selected.

```
--- Calculating Process Suitability Index (PSI) ---
Labour_Cost_Index converted to 'Labour_Cost_Index_Numeric' successfully.
       Process       Mode      mean  Pass Rate  Labour_Cost_Index_Numeric  \
3          SAW  Automated  26.425950 100.000000                       -1.0
0        CoBot  Automated  22.454708  98.888889                       -1.0
1           PT  semi_auto  18.043550  80.000000                        0.0
2  Manual_FCAW     Manual   8.296737  78.947368                        1.0
        PSI
3  1.000000
0  0.722379
1  0.335052
2  0.000000
```

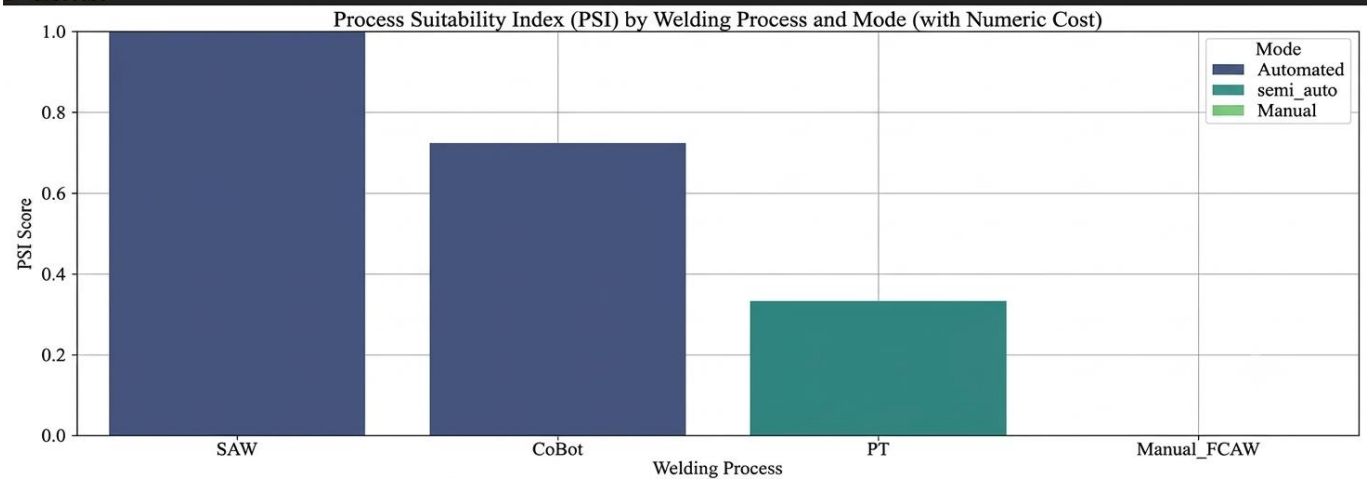


Fig. 20 Process Suitability Index (PSI) by welding process and mode (with numeric cost)

Structure Item	Welded To	Joint Type	Proposed Weld Type
DOUBLE BOTTOM			
Centre Girder	Keel Plate	T-Joint	Double Continuous
Centre Girder	Deck	T-Joint	Double Continuous
Side Girder	Bottom Shell	T-Joint	Double Continuous
Floors	Shell Plating	T-Joint	Double Continuous
Web Frame	Shell Plating	T-Joint	Double Continuous
TANK BOUNDARIES			
W.T Center Girder	Keel Plate	T-Joint	Double Continuous
W.T Side Girder	Shell Plate	T-Joint	Double Continuous
W.T Floors	Shell, Keel, Stiffeners	T-Joint	Double Continuous
MACHINERY SPACES			
Floors & Girders	Shell	T-Joint	Double Continuous
Main Engine.	Face Plate	Butt Joint	Full Penetration
Main Engine.	Hull Structure	Butt/T-Joint	Full Penetration
SIDE STRUCTURE			
Side Longitudinal	Shell Plating	T-Joint	Staggered Intermittent
Web Frames	Shell Plating	T-Joint	Chain/Staggered
Web Frames	Side Stringer	T-Joint	Double Continuous
DECK STRUCTURE			
Deck	Shell	Corner Joint	Double Continuous
Deck Longitudinal	Deck	T-Joint	Double Continuous
Deck Beams	Deck	T-Joint	Double Continuous
Deck Girders	Deck	T-Joint	Double Continuous
Deck Longitudinal	Decks	T-Joint	Staggered Intermittent
Deck Beams	Decks	T-Joint	Chain Intermittent
Pillars	Doubler Plate	Butt/Cruciform	Double Continuous

Fig. 21 Decision framework for proposed weld type

Process	Linear Meters/Hour (Avg)	Efficiency Gain vs. Manual
Manual FCAW	1.0x	Base Line
Cobot	1.8x	80% (Due to continuous reach)
Flux Track	2.5x	150% (Constant travel speed)
Mogi	3.2x	220% (Multi-pass capability)
SAW	5.0x+	400%+ (High deposition rate)

Fig. 22 Productivity of the processes

Structure Item	Welded To	Joint Type	Suggested Process
HULL & BOTTOM			
Centre / Side Girders	Keel & Shell Plates	T-Joint	SAW (Mechanized)
Floors / WT Floors	Shell Plating	T-Joint	SAW / Flux Track
Main Engine Foundation	Hull Structure	Butt / T-Joint (FP)	Manual FCAW (Critical)
SIDE & SHELL			
Side Longitudinal	Shell Plating	T-Joint	Flux Track
Web Frames	Shell Plating	T-Joint	Flux Track / Manual
Web Frames	Side Stringers	T-Joint	Manual FCAW
DECK & INTERNAL			
Deck Longitudinal	Deck Plating	T-Joint	Mogi (Auto-carriage)
Deck Beams / Girders	Deck Plating	T-Joint	Mogi / Flux Track
Strength Deck	Shell (Gunwale)	Corner Joint	Flux Track / Manual
Pillars	Doubler Plates	T-Joint	Manual FCAW
BULKHEADS & SUPERSTRUCTURE			
Bulkhead Boundaries	Shell / Deck	T-Joint	Manual FCAW
Vertical Webs	BHD Plate	T-Joint	Manual FCAW (Vertical)
Web Frames / Brackets	Face Plates	T-Joint	Cobot
Stiffeners	BHD / Side Shell	T-Joint	Cobot / Mogi
FITTINGS			
Sea-Chest	Shell	Butt Joint (FP)	Manual FCAW
Bulwark Stays	Deck / Bulwark	T-Joint	Cobot / Manual

Fig. 23 Suggested framework for welding process selection from the simulation performed

The data shows a clear preference for automation. SAW leads with peak productivity, a 100% pass rate, and minimal labour costs. In contrast, Manual FCAW ranks lowest due to slow speeds and higher defect rates. Ultimately, increasing automation directly improves process suitability by optimizing output quality while reducing expensive manual labour. If a facility is currently using Manual FCAW, transitioning even to a Semi-Auto (FT) or CoBot system would provide a massive jump in "suitability" by cutting labour costs and boosting output quality. The data suggests that manual processes aren't just slower; they are also more prone to defects (lower pass rates), which likely leads to expensive rework.

7. Sensitivity and Scenario Analysis

By establishing this framework, we achieve three critical goals:

- Process Optimization: It allows us to match the right welding technology-whether it's a Cobot for complex web frames or SAW for long butt welds-to the specific geometry of the part. As shown in the productivity data, selecting the wrong process can mean the difference between a 1.0x baseline speed and a 5.0x efficiency gain.
- Cost and Resource Management: The framework helps justify the capital investment in automation. By predicting the linear meters per hour for different components, we can accurately estimate project timelines and labour costs, ensuring we meet delivery schedules.
- Consistency and Quality Control: Automation reduces the "human variability" factor. This framework ensures that high-stress areas, like H-beam stiffeners or plate joints, are welded with the constant travel speeds and deposition rates required to minimize defects and thermal distortion.

8. Conclusions

The evaluation of process efficiency for welding in the applications of ship building is investigated in this study by integrating Monte Carlo simulation, statistical variability analysis and transient thermal analysis. To select suitable parameters of welding, a quantitative decision framework has been developed by incorporating productivity, weld quality, heat input and operational cost.

Broadly, this study developed a framework that, in shipbuilding to improve the productivity, quality and resource utilization, a more reliable approach is being established by selecting the process parameters of welding based on joint geometry, fabrication complexity and performance parameters.

The specific conclusions are as follows:

1. Based on joint configurations and fabrication requirements, three different methods of welding processes viz., manual, semi-automated and cobot-assisted welding processes were compared systematically by proposing a new framework.
2. Monte Carlo simulation highlights process variability and productivity differences, while correlation analysis indicates a negative relationship between heat input and productivity ($r = -0.5513$) and a positive relationship between productivity and RT quality ($r = 0.2532$).

3. Transient thermal analysis using the Goldak double-ellipsoidal heat-source model provides insights into temperature distribution and heat propagation, emphasizing the importance of controlling heat input to minimize thermal inconsistencies.
4. The Process Suitability Index (PSI) identifies SAW as the most suitable among the evaluated processes, considering productivity, RT quality, heat input and operational cost.
5. The framework facilitates improved production planning, resource allocation and project timeline estimation, although further validation using actual industrial welding datasets is required.

8.1. Future Scope

Integration of real-time welding data, machine learning and digital-twin technologies can transform the proposed framework into an intelligent decision-support system for adaptive welding-process selection and advanced shipbuilding operations.

Acknowledgements

The authors would like to thank the Management & Principal of Vasavi College of Engineering, Hyderabad, for the research facilities provided to carry out this work.

References

[1] Khaled Younis Benyounis, and Abdul Ghani Olabi, "Optimization of Different Welding Processes using Statistical and Numerical Approaches-A Reference Guide," *Advances in Engineering Software*, vol. 39, no. 6, pp. 483-496, 2008. [CrossRef] [Google Scholar] [Publisher Link]

[2] Mayank Srinivasamurthy, "*Comparative Study of Robotic and Manual Welding in a Low Volume-High Mix Manufacturing Environment: Case Study of JR Test 3*," Master's Thesis, Minnesota State University, Mankato, USA, pp. 1-13, 2024. [Google Scholar]

[3] Jinfeng Liu et al., "Prediction and Optimization Method for Welding Quality of Components in Ship Construction," *Scientific Reports*, vol. 14, no. 1, pp. 1-18, 2024. [CrossRef] [Google Scholar] [Publisher Link]

[4] Hui Zhang et al., "Experimental and Simulation Study on Welding Characteristics and Parameters of Gas Metal Arc Welding for Q345qD Thick-Plate Steel," *Materials*, vol. 16, no. 17, pp. 1-14, 2023. [CrossRef] [Google Scholar] [Publisher Link]

[5] Qinglei Zhang et al., "Process Simulation and Optimization of Arc Welding Robot Workstation based on Digital Twin," *Machines*, vol. 11, no. 1, pp. 1-21, 2023. [CrossRef] [Google Scholar] [Publisher Link]

[6] Anish Pandey et al., "An Analysis of the Efficiency and Accuracy of Manual and Autonomous Four-Wheeled Linear Welding Across Various Parameters," *Discover Mechanical Engineering*, vol. 4, no. 1, pp. 1-21, 2025. [CrossRef] [Google Scholar] [Publisher Link]

[7] Hongwei Sun et al., "Optimization of Laser-MAG Hybrid Welding Parameters of Ship Steel based on Response Surface Methodology," *Materials*, vol. 15, no. 12, pp. 1-14, 2022. [CrossRef] [Google Scholar] [Publisher Link]

[8] Bhoopathy Bhaskaran, "Mechanization of Production Process in Shipbuilding: A Review," *Journal of Engineering and Applied Sciences*, vol. 13, no. 4, pp. 857-860, 2018. [Publisher Link]

[9] Eda Turan, Tarık Koçal, and Kaan Ünlügençoğlu, "Welding Technologies in Shipbuilding Industry," *The Online Journal of Science and Technology*, vol. 1, no. 4, pp. 24-30, 2011. [Google Scholar] [Publisher Link]

[10] Z. Samad, N.M. Nor, and E.R.I. Fauzi, "Thermo-Mechanical Simulation of Temperature Distribution and Prediction of Heat-Affected Zone Size in MIG Welding Process on Aluminium Alloy EN AW 6082-T6," *IOP Conference Series: Materials Science and Engineering*, vol. 530, no. 1, pp. 1-14, 2019. [CrossRef] [Google Scholar] [Publisher Link]

[11] Yannik Hahn et al., "Metal Arc Welding," 2023. [Google Scholar]

[12] V. Ravisankar, Visvalingam Balasubràmanian, and C. Muralidharan, "Selection of Welding Process to Fabricate Butt Joints of High Strength Aluminium Alloys using Analytic Hierarchic Process," *Materials and Design*, vol. 27, no. 5, pp. 373-380, 2006. [CrossRef] [Google Scholar] [Publisher Link]

[13] Mostafa Jafarian, and S. Ebrahim Vahdat, "A Fuzzy Multi-Attribute Approach to Select the Welding Process at High Pressure Vessel Manufacturing," *Journal of Manufacturing Processes*, vol. 14, no. 3, pp. 250-256, 2012. [CrossRef] [Google Scholar] [Publisher Link]

[14] Abhijit Sarkar et al., "Optimization of Process Parameters of Submerged Arc Welding by using Grey–Fuzzy-based Taguchi Method for AISI 1518 Grade Steel," *Proceedings of the Institution of Mechanical Engineers, Part B: Journal of Engineering Manufacture*, vol. 228, no. 11, pp. 1491-1500, 2014. [CrossRef] [Google Scholar] [Publisher Link]

[15] Pankaj Sharma, and Sachin Mohala, "Parametric Optimization of Submerged Arc Welding Process Parameters by Response Surface Methodology," *Materials Today: Proceedings*, vol. 24, pp. 673-682, 2020. [CrossRef] [Google Scholar] [Publisher Link]

[16] Małgorzata Ostromęcka, "Application of Taguchi Method in Welding Technology," *Welding Technology Review*, vol. 89, no. 9, pp. 22-25, 2017. [Google Scholar] [Publisher Link]

[17] Samson Jerold Samuel Chelladurai et al., "Optimization of Process Parameters using Response Surface Methodology: A Review," *Materials Today: Proceedings*, vol. 37, pp. 1301-1304, 2021. [CrossRef] [Google Scholar] [Publisher Link]

[18] D. Katherasan et al., "Flux Cored Arc Welding Parameter Optimization using Particle Swarm Optimization Algorithm," *Procedia Engineering*, vol. 38, pp. 3913-3926, 2012. [CrossRef] [Google Scholar] [Publisher Link]

[19] M.A. Moradpour, S.H. Hashemi, and K. Khalili, "Multi-objective Optimization of Welding Parameters in Submerged Arc Welding of API X65 Steel Plates," *Journal of Iron and Steel Research International*, vol. 22, no. 9, pp. 870-878, 2015. [CrossRef] [Google Scholar] [Publisher Link]

[20] John Goldak, Aditya Chakravarti, and Malcolm Bibby, "A New Finite Element Model for Welding Heat Sources," *Metallurgical Transactions B*, vol. 15, no. 2, pp. 299-305, 1984. [CrossRef] [Google Scholar] [Publisher Link]

[21] D. Gery, Hui Long, and Paul G. Maropoulos, "Effects of Welding Speed, Energy Input and Heat Source Distribution on Temperature Variations in Butt Joint Welding," *Journal of Materials Processing Technology*, vol. 167, no. 2-3, pp. 393-401, 2005. [CrossRef] [Google Scholar] [Publisher Link]

[22] Dean Deng, Hidekazu Murakawa, and Wei Liang, "Numerical Simulation of Welding Distortion in Large Structures," *Computer Methods in Applied Mechanics and Engineering*, vol. 196, no. 45-48, pp. 4613-4627, 2007. [CrossRef] [Google Scholar] [Publisher Link]

[23] Liam Gannon et al., "Effect of Welding Sequence on Residual Stress and Distortion in Flat-Bar Stiffened Plates," *Marine Structures*, vol. 23, no. 3, pp. 385-404, 2010. [CrossRef] [Google Scholar] [Publisher Link]

[24] Guangming Fu et al., "Influence of the Welding Sequence on Residual Stress and Distortion of Fillet Welded Structures," *Marine Structures*, vol. 46, pp. 30-55, 2016. [CrossRef] [Google Scholar] [Publisher Link]

[25] Navid Azad, Mehdi Iranmanesh, and Armin Rahmati Darvazi, "A Study on the Effect of Welding Sequence on Welding Distortion in Ship Deck Structure," *Ships and Offshore Structures*, vol. 15, no. 4, pp. 355-367, 2020. [CrossRef] [Google Scholar] [Publisher Link]

[26] Sufian Imam Wahidi et al., "Structural Optimisation for Minimising Weight and Welding in Confined Shipbuilding Spaces: Enhancing Safety and Reducing Costs," *Ocean Engineering*, vol. 341, pp. 1-15, 2025. [CrossRef] [Google Scholar] [Publisher Link]